SMALL x PHYSICS IN DEEP INELASTIC LEPTON SCATTERING*,**

J. KWIECIŃSKI

Department of Physics, University of Durham
Durham, United Kingdom
and
Department of Theoretical Physics
H. Niewodniczański Institute of Nuclear Physics
Radzikowskiego 152, 31-342 Kraków, Poland ***

(Received November 28, 1995)

The perturbative QCD predictions concerning deep inelastic scattering at low x are summarized. The theoretical framework based on the leading log $1/x$ resumation and k_t factorization theorem is described. The role of studying final states in deep inelastic scattering for revealing the details of the underlying dynamics at low x is emphasized and some dedicated measurements, like deep inelastic scattering accompanied by an energetic jet, the measurement of the transverse energy flow and deep inelastic diffraction, are briefly discussed.

PACS numbers: 11.55.Jy, 12.38.Bx

1. Introduction

It has been known for quite some time [1, 2] that perturbative QCD predicts several new phenomena to occur when the parameter x specifying the longitudinal momentum fraction of a hadron carried by a parton (*i.e.* by a quark or by a gluon) becomes very small. The main expectation was that the gluon and quark densities should strongly grow in this limit eventually leading to the parton saturation effects [1–4]. This increase of parton

* Presented at the XXXV Cracow School of Theoretical Physics, Zakopane, Poland, June 4–14, 1995.

** This research has been supported in part by the Polish State Committee for Scientific Research grant 2 P302 062 04 and the EU under contracts n0. CHRX-CT92-0004/CT93-357.

*** Permanent address.

distributions implies similar increase of the deep inelastic lepton - proton scattering structure function F_2 with the decreasing Bjorken parameter x [6] and the experimental data from HERA are consistent with this prediction [7, 8]. The Bjorken parameter x is as usual defined as $x = Q^2/(2pq)$ where

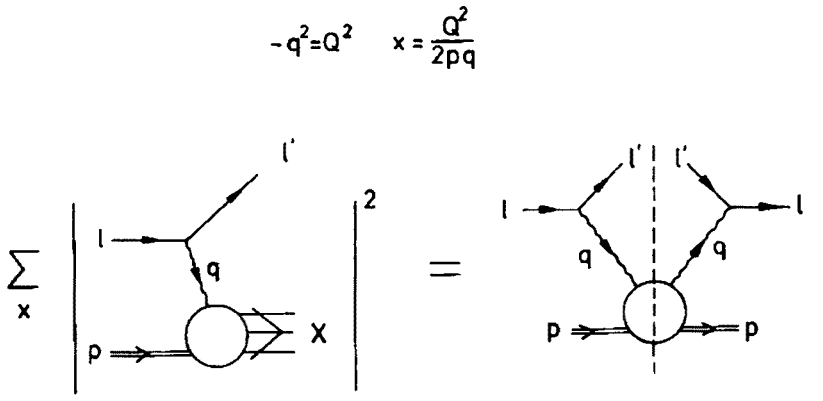

Fig. 1. Kinematics of inelastic lepton-nucleon scattering in the one photon exchange approximation and its relation through the optical theorem to Compton scattering of the virtual photon. p and q denote the four momenta of the nucleon and of the virtual photon, respectively.

The growth of structure functions with decreasing parameter x is much stronger than that which would follow from the expectations based on the "soft" pomeron exchange mechanism with the soft pomeron intercept $\alpha_{\text{soft}} \approx 1.08$ as determined from the phenomenological analysis of total hadronic and real photoproduction cross-sections [9].

Small x behaviour of structure functions for fixed Q^2 reflects the high energy behaviour of the virtual Compton scattering total cross-section with increasing total CM energy squared W^2 since $W^2 = Q^2(1/x - 1)$. The Regge pole exchange picture [10] is, therefore, quite appropriate for the theoretical description of this behaviour. The high energy behaviour which follows from perturbative QCD is often referred to as being related to the "hard" pomeron in contrast to the soft pomeron describing the high energy behaviour of hadronic and photoproduction cross-sections.

The inelastic lepton–nucleon scattering is related through the one photon exchange mechanism illustrated in Fig. 1 to the Compton scattering of virtual photons. In Fig. 2 we summarize the present experimental situation

on the variation of the total virtual Compton scattering cross-section with total CM energy W for different photon virtualities Q^2 which range from the real photoproduction ($Q^2 = 0$) to the deep inelastic region [12]. The change of high energy behaviour with the scale Q^2 is evidently present in the data.

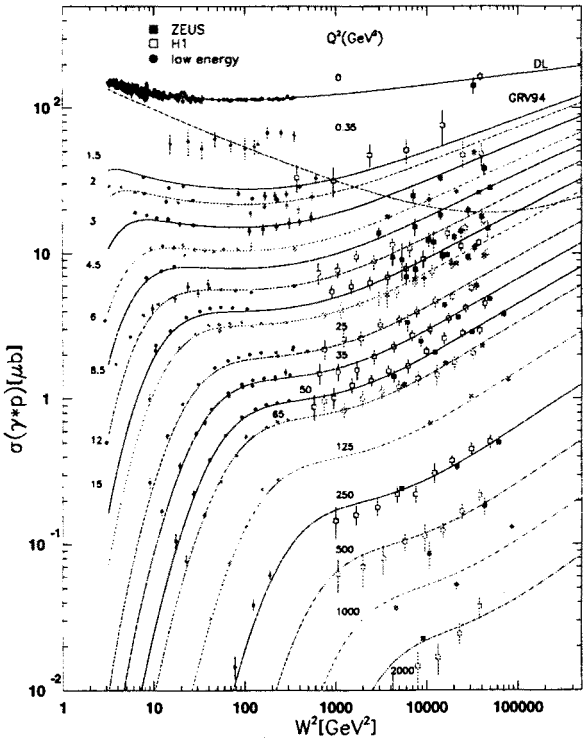

Fig. 2. The total virtual photon cross-section plotted as a function of W^2 for different values of the photon virtuality Q^2. The curves correspond to the theoretical parametrizations [32, 11]. The figure is taken from Ref. [12].

The purpose of this lecture is to summarize briefly the QCD expectations for the deep inelastic scattering at low x. In the next section we recall the parton model and the Regge pole model expectations for the description of the small x behaviour of deep inelastic scattering structure functions. Section 3 is devoted to the description of the QCD improved parton model based on the Altarelli–Parisi evolution equations and the collinear factorization [13, 14]. We discuss the small x behaviour of structure functions which follows from this formalism. In Section 4 we summarize the results based on the leading $\ln 1/x$ resumation which is provided by the Balitzkij, Fadin, Kuraev, Lipatov (BFKL) equation and k_t factorization. We also briefly

discuss the Catani, Ciafaloni, Fiorani Marchesini (CCFM) equation based on the angular ordering of gluon emission [15, 16]. This equation embodies the BFKL $\ln 1/x$ resumation and the conventional QCD evolution in the regions of small and large values of x, respectively. Section 5 is devoted to a brief discussion of the dedicated measurements of the hadronic final state in deep inelastic scattering for revealing the dynamical QCD expectations at low x. Section 6 contains a brief summary and conclusions.

2. Parton model description of deep inelastic lepton scattering

The inelastic lepton–nucleon scattering is related through the one photon exchange mechanism and through the optical theorem to the imaginary part of the forward Compton scattering amplitude of virtual photons (see Fig. 1). The latter is defined by the tensor $W^{\mu\nu}$ [18, 19]:

$$W^{\mu\nu}(p,q) = \frac{F_1(x,Q^2)}{M}\left(-g_{\mu\nu} + \frac{q^\mu q^\nu}{q^2}\right) + \frac{F_2(x,Q^2)}{M(pq)}\left(p^\mu - \frac{pq}{q^2}q^\mu\right)\left(p^\nu - \frac{pq}{q^2}q^\nu\right). \tag{1}$$

In this equation p denotes the four momentum of the nucleon, $Q^2 = -q^2$ where q is the four momentum transfer between the leptons, $x = Q^2/(2pq)$ the Bjorken scaling variable and M is the nucleon mass. The functions $F_{1,2}(x,Q^2)$ are the nucleon structure functions. These structure functions are directly related to the total cross-sections σ_L and σ_T corresponding to the longitudinally and transversely polarized virtual photons, respectively:

$$F_2 = \frac{Q^2}{4\pi^2\alpha}(\sigma_T + \sigma_L), \tag{2}$$

$$F_L = F_2 - 2xF_1 = \frac{Q^2}{4\pi^2\alpha}\sigma_L. \tag{3}$$

The differential cross-section describing inelastic lepton scattering is related in the following way to the structure functions F_2 and F_1:

$$\frac{d^2\sigma(x,Q^2)}{dxdQ^2} = \frac{4\pi\alpha^2}{Q^4}\left[(1-y)\frac{F_2(x,Q^2)}{x} + y^2F_1(x,Q^2)\right], \tag{4}$$

where $y = pq/p_lp$ with p_l denoting the four-momentum of the incident lepton.

The deep inelastic regime is defined as the region where both Q^2 and $2pq$ are large and their ratio, x, is fixed. It is assumed that in this region the

deep inelastic scattering reflects the (elastic) lepton scattering on (point-like) quarks and antiquarks, as illustrated by the "hand-bag" diagram of Fig. 3, with the virtuality k^2 of the quark (antiquark) being limited. The "hand- bag" diagram for virtual Compton scattering together with the limitation of the virtuality k^2 form the basis of the (covariant) parton model which leads to Bjorken scaling (*i.e.* $F_2(x, Q^2) \to F_2(x)$) [20]. In the infinite momentum frame the Bjorken variable x acquires the meaning of the momentum fraction of the parent nucleon carried by a probed quark (antiquark). For spin 1/2 partons the structure function F_L vanishes in the deep inelastic region- this being a straightforward consequence of the limitation of the quark transverse momentum [18, 19].

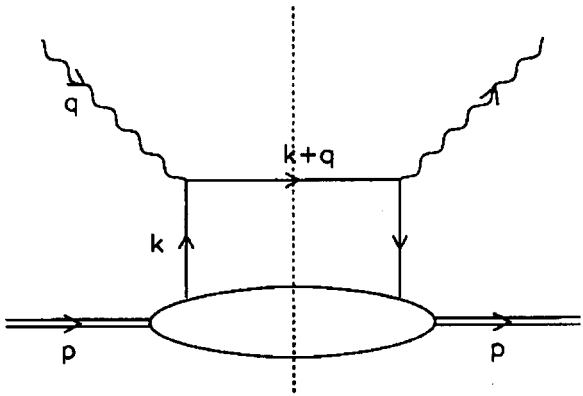

Fig. 3. The hand-bag diagram for the virtual Compton scattering on a nucleon; k denotes the four momentum of the struck quark (antiquark). At high Q^2 and in the infinite momentum frame of the nucleon $k \approx xp$ where x is the Bjorken scaling variable.

In the parton model the structure function F_2 becomes directly related to the quark and antiquark distributions $q_i(x)$ and $\bar{q}_i(x)$ in a nucleon

$$F_2 = x \sum_i e_i^2 [q_i(x) + \bar{q}_i(x)] , \tag{5}$$

where e_i is the charge of the quark carrying flavour "i". At small x (*i.e.* for $2pq \gg Q^2$) one can use the Regge pole model for parametrizing the high energy behaviour of the total cross-sections $\sigma_{T,L}$ and obtain, using Eq. (2), the following parametrization of the structure function $F_2(x, Q^2)$:

$$F_2 = \sum_i \tilde{\beta}_i x^{1-\alpha_i(0)} . \tag{6}$$

The relevant reggeons are those which can couple to two (virtual) photons. The (singlet) part of the structure function F_2 is controlled at small x by the pomeron exchange, while the non-singlet part $F_2^{NS} = F_2^p - F_2^n$ by the A_2 reggeon. From equations (6) and (5) one gets the corresponding Regge behaviour of quark (antiquark) distributions.

3. Small x limit of parton distributions in the QCD — improved parton model

The Bjorken scaling (*i.e.* independence of the structure functions of Q^2) is violated by the elementary QCD interactions and the parton (*i.e.* the quark, antiquark and gluon distributions) acquire Q^2 dependence. Their change with Q^2 is described by the Altarelli–Parisi evolution equations [13, 14]. In the leading $\ln(Q^2)$ approximation which resumes the leading powers of $\alpha_s ln(Q^2)$ the Eq. (5) still holds, although the quark (and antiquark) distributions are now scale dependent. This scale dependence comes from the fact that the quark (antiquark) virtuality k^2 in the "hand-bag" diagram of Fig. 3 is no longer limited as in the "naive" parton model. This lack of limitation of k^2 is the result of the (point-like) elementary QCD interactions. The dominant region from which the scaling violations come is now $k_0^2 \ll k^2 \ll Q^2$, where k_0^2 is some infrared cut-off. Beyond the leading $\ln(Q^2)$ approximation the Eq. (5) acquires $O(\alpha_s)$ corrections which are, however, (by definition) absent in the so called deep inelastic (DIS) scheme.

At small x the dominant role is played by the gluons and so for simplicity we shall limit ourselves to the following system of the evolution equations:

$$Q^2 \frac{dq(x,Q^2)}{dQ^2} = \int_x^1 \frac{dz}{z} P_{qg}(z, \alpha_s(Q^2)) g(\frac{x}{z}, Q^2), \tag{7}$$

$$Q^2 \frac{dg(x,Q^2)}{dQ^2} = \int_x^1 \frac{dz}{z} P_{gg}(z, \alpha_s(Q^2)) g(\frac{x}{z}, Q^2), \tag{8}$$

where $q(x,Q^2)$ and $g(x,Q^2)$ are the scale dependent quark and gluon distributions, respectively. The splitting functions $P_{ij}(z, \alpha_s(Q^2))$ can be expanded in the perturbative series of the QCD coupling $\alpha_s(Q^2)$. In leading order

$$P_{ij}(z, \alpha_s(Q^2)) = \frac{\alpha_s(Q^2)}{2\pi} P_{ij}^{(0)}(z). \tag{9}$$

In an axial gauge the leading order evolution equations sum ladder diagrams with ordered longitudinal and strongly ordered transverse momenta along the chain.

The evolution equations can be solved in a closed form for the moment functions $\bar{h}(\omega, Q^2)$ of the parton distributions $h(x, Q^2)$

$$\bar{h}(\omega, Q^2) = \int_0^1 \frac{dx}{x} x^\omega x h(x, Q^2), \tag{10}$$

where $h(x, Q^2)$ denotes the gluon or quark (antiquark) distribution. The distribution $h(x, Q^2)$ is related by the inverse transform to the moment function

$$h(x, Q^2) = \frac{1}{2\pi i} \int_{c-i\infty}^{c+i\infty} d\omega x^{\omega-1} \bar{h}(\omega, Q^2), \tag{11}$$

where the integration contour is located to the right of the leading (*i.e.* rightmost) singularity of the moment function $\bar{h}(\omega, Q^2)$ in the ω complex plane. The use of moments is, therefore, useful for understanding the small x behaviour which is controlled by the leading singularity of the moment functions in the ω plane.

The solution of the counterpart of the evolution equation (8) for the moment function $\bar{g}(\omega, Q^2)$

$$\bar{g}(\omega, Q^2) = \int_0^1 \frac{dx}{x} x^\omega x g(x, Q^2) \tag{12}$$

is of the form:

$$\bar{g}(\omega, Q^2) = \bar{g}(\omega, Q_0^2) \exp\left[\int_{Q_0^2}^{Q^2} \frac{dq^2}{q^2} \gamma_{gg}(\omega, \alpha_s(q^2))\right] \tag{13}$$

and, similarly the quark distributions "driven by the gluon" are given by:

$$Q^2 \frac{d\bar{q}(\omega, Q^2)}{dQ^2} = \gamma_{qg}(\omega, \alpha_s(Q^2)) \bar{g}(\omega, Q_0^2) \exp\left[\int_{Q_0^2}^{Q^2} \frac{dq^2}{q^2} \gamma_{gg}(\omega, \alpha_s(q^2))\right]. \tag{14}$$

The anomalous dimensions $\gamma_{ij}(\omega, \alpha_s(Q^2))$ are moments of the splitting functions $P_{ij}(z, \alpha_s(q^2))$

$$\gamma_{ij}(\omega, \alpha_s(Q^2)) = \int_0^1 \frac{dz}{z} z^\omega z P_{ij}(z, \alpha_s(Q^2)). \tag{15}$$

In the leading order

$$\int_{Q_0^2}^{Q^2} \frac{dq^2}{q^2} \gamma_{gg}(\omega, \alpha_s(q^2)) = \gamma_{gg}^{(0)}(\omega) \xi(Q^2, Q_0^2), \tag{16}$$

where

$$\xi(Q^2, Q_0^2) = \int_{Q_0^2}^{Q^2} \frac{dq^2}{q^2} \frac{\alpha_s(q^2)}{2\pi} \sim \log \left(\frac{\log(\frac{Q^2}{\Lambda^2})}{\log(\frac{Q_0^2}{\Lambda^2})} \right), \tag{17}$$

and $\gamma_{gg}^{(0)}(\omega)$ is the moment of $P_{gg}(z)$.

The singularities of the moment function $\bar{g}(\omega, Q^2)$ in the ω plane are present both in the anomalous dimension $\gamma_{gg}(\omega, \alpha_s(q^2))$ as well as in the moment of the input nonperturbative gluon distribution $\bar{g}(\omega, Q_0^2)$, see (13). The small x behaviour of the gluon distributions is controlled by the leading singularity. The same singularity should also control the small x behaviour of the (sea) quark distributions through the $g \to q\bar{q}$ transitions which, within the QCD evolution formalism, are described by Eq. (14). In leading order, the anomalous dimension $\gamma_{gg}(\omega, \alpha_s(q^2))$ has a pole at $\omega = 0$ since $P_{gg}^0(z) \sim 6/z$ at small z. It leads to the essential singularity of the moment function $\bar{g}(\omega, Q^2)$ at $\omega = 0$ (see Eq. (13)). This essential singularity remains the leading one provided that the starting gluon distribution $x\bar{g}(x, Q_0^2)$ behaves (at most) as a constant at small x. One gets then the following "double logarithmic behaviour" for the gluon distribution at small x:

$$xg(x, Q^2) \sim \exp\left(2\sqrt{6\xi(Q^2, Q_0^2) \ln\left(\frac{1}{x}\right)} \right) \tag{18}$$

with similar behaviour for the sea quark distributions. If a more singular behaviour is taken for the input $xg(x, Q_0^2)$ then it remains stable against leading order QCD evolution in Q^2.

4. The BFKL pomeron and QCD predictions for the small x behaviour of the deep inelastic scattering structure functions

The QCD improved parton model in which the splitting functions $P_{ij}(z)$ are computed at fixed order of their perturbative expansions is incomplete in the small x region. In this region the perturbative terms generate powers of $\ln(1/x)$ and we should, at least, resume the powers of $\alpha_s \ln(1/x)$ *i.e.* to

consider the leading $ln(1/x)$ approximation. The basic dynamical quantity now is the unintegrated gluon distribution $f(x, Q_t^2)$ where x denotes the momentum fraction of a parent hadron carried by a gluon and Q_t its transverse momentum. The unintegrated distribution $f(x, Q_t^2)$ is related in the following way to the more familiar scale dependent gluon distribution $g(x, Q^2)$:

$$xg(x, Q^2) = \int^{Q^2} \frac{dQ_t^2}{Q_t^2} f(x, Q_t^2) . \tag{19}$$

In the leading $\ln(1/x)$ approximation the unintegrated distribution $f(x, Q_t^2)$ satisfies the BFKL equation [5] which has the following form:

$$f(x, Q_t^2) = f^0(x, Q_t^2) + \bar{\alpha}_s \int_x^1 \frac{dx'}{x'} \int \frac{d^2q}{\pi q^2}$$
$$\times \left[\frac{Q_t^2}{(q + Q_t)^2} f(x', (q + Q_t)^2) - f(x', Q_t^2) \Theta(Q_t^2 - q^2) \right] , \tag{20}$$

where

$$\bar{\alpha}_s = \frac{3\alpha_s}{\pi} . \tag{21}$$

The first and the second terms on the right hand side of Eq. (20) correspond to real gluon emission with q being the transverse momentum of the emitted gluon, and to the virtual corrections, respectively. $f^0(x, Q_t^2)$ is a suitably defined inhomogeneous term.

After resuming the virtual corrections and "unresolvable" gluon emissions ($q^2 < \mu^2$) where μ is the resolution defining the "resolvable" radiation, equation (20) can be rearranged into the following "folded" form:

$$f(x, Q_t^2) = \hat{f}^0(x, Q_t^2) + \bar{\alpha}_s \int_x^1 \frac{dx'}{x'} \int \frac{d^2q}{\pi q^2} \Theta(q^2 - \mu^2)$$
$$\times \Delta_R\left(\frac{x}{x'}, Q_t^2\right) \frac{Q_t^2}{(q + Q_t)^2} f(x', (q + Q_t)^2) + O\frac{\mu^2}{Q_t^2} , \tag{22}$$

where Δ_R which screens the $1/z$ singularity is given by:

$$\Delta_R(z, Q_t^2) = z^{\bar{\alpha}_s \ln(Q_t^2/\mu^2)} = \exp\left(-\bar{\alpha}_s \int_z^1 \frac{dz'}{z'} \int_{\mu^2}^{Q_t^2} \frac{dq^2}{q^2} \right) , \tag{23}$$

and

$$\hat{f}^0(x,Q_t^2) = \int_x^1 \frac{dx'}{x'} \Delta_R(\frac{x}{x'},Q_t^2) \frac{df^0(x',Q_t^2)}{d\ln(1/x')}. \tag{24}$$

Equation (22) sums the ladder diagrams (see Fig. 4) with the reggeized gluon exchange along the chain with the gluon trajectory $\alpha_G(Q_t^2) = 1 - \frac{\bar{\alpha}_s}{2}\ln(Q_t^2/\mu^2)$.

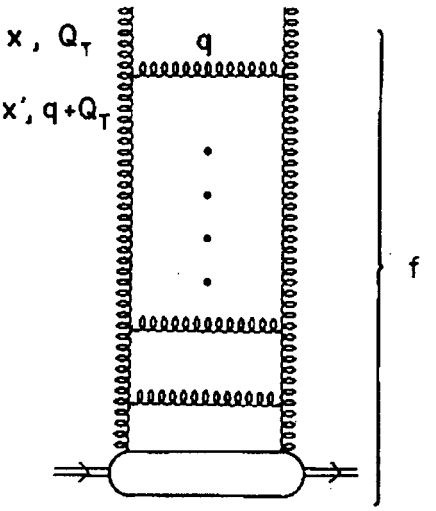

Fig. 4. Diagrammatic representation of the BFKL equation (22).

For the fixed coupling case Eq. (20) can be solved analytically and the leading behaviour of its solution at small x is given by the following expression:

$$f(x,Q_t^2) \sim (Q_t^2)^{\frac{1}{2}} \frac{x^{-\lambda_{\rm BFKL}}}{\sqrt{ln(\frac{1}{x})}} \exp\left(-\frac{\ln^2(Q_t^2/\bar{Q}^2)}{2\lambda''\ln(1/x)}\right) \tag{25}$$

with

$$\lambda_{\rm BFKL} = 4\ln(2)\bar{\alpha}_s, \tag{26}$$

$$\lambda'' = \bar{\alpha}_s 28\zeta(3), \tag{27}$$

where the Riemann zeta function $\zeta(3) \approx 1.202$. The parameter $\bar{Q}$ is of nonperturbative origin.

The quantity $1+\lambda_{\mathrm{BFKL}}$ is equal to the intercept of the so-called BFKL pomeron. Its potentially large magnitude (~ 1.5) should be contrasted with the intercept $\alpha_{\mathrm{soft}} \approx 1.08$ of the (effective) "soft" pomeron which has been determined from the phenomenological analysis of the high energy behaviour of hadronic and photoproduction total cross-sections [9].

In practice one introduces the running coupling $\bar{\alpha}_s(Q_t^2)$ in the BFKL equation (20). This requires introduction of the infrared cut-off that would prevent entering the infrared region where the coupling becomes large. The effective intercept λ_{BFKL} found by numerically solving the equation depends weakly on the magnitude of this cut-off [23].

The solution (25) of the BFKL equation is obtained most directly by solving from the solution of the corresponding equation for the moment function

$$\bar{f}(\omega, Q_t^2) = \int_0^1 \frac{dx}{x} x^\omega f(x, q_t^2)\,, \tag{28}$$

$$\bar{f}(\omega, Q_t^2) = \bar{f}^0(\omega, Q_t^2) + \frac{\bar{\alpha}_s}{\omega} \int \frac{d^2q}{\pi q^2} \times \left[\frac{Q_t^2}{(q+Q_t)^2} \bar{f}(\omega, (q+Q_t)^2) - \bar{f}(\omega, Q_t^2)\Theta(Q_t^2 - q^2) \right]. \tag{29}$$

This equation can be diagonalized by a Mellin transform and its solution for the Mellin transform $\tilde{f}(\omega, \gamma)$ of the moment function $\bar{f}(\omega, Q_t^2)$ is:

$$\tilde{f}(\omega, \gamma) = \frac{\tilde{f}^0(\omega, \gamma)}{1 - \frac{\bar{\alpha}_s}{\omega}\tilde{K}(\gamma)}\,, \tag{30}$$

where

$$\tilde{K}(\gamma) = 2\Psi(1) - \Psi(\gamma) - \Psi(1-\gamma) \tag{31}$$

is the Mellin transform of the kernel of Eq. (29). The function $\Psi(z)$ is the logarithmic derivative of the Euler Γ function. The Mellin transform $\tilde{f}(\omega, \gamma)$ is defined as below:

$$\tilde{f}(\omega, \gamma) = \int_0^\infty \frac{dQ_t^2}{Q_t^2} (Q_t^2)^{-\gamma} \bar{f}(\omega, Q_t^2)\,, \tag{32}$$

and hence the function $\bar{f}(\omega, Q_t^2)$ is related to $\tilde{f}(\omega, \gamma)$ through the inverse Mellin transform

$$\bar{f}(\omega, Q_t^2) = \frac{1}{2\pi i} \int_{1/2-i\infty}^{1/2+i\infty} d\gamma (Q_t^2)^\gamma \tilde{f}(\omega, \gamma)\,. \tag{33}$$

The poles of $\tilde{f}(\omega,\gamma)$ in the γ plane define the anomalous dimensions of the moment function $\bar{f}(\omega,Q_t^2)$ [21]. The (leading twist) anomalous dimension $\gamma_{gg}(\omega,\bar{\alpha}_s)$ of $\bar{f}(\omega,Q_t^2)$ gives the following behaviour of $\bar{f}(\omega,Q_t^2)$ at large Q_t^2

$$\bar{f}(\omega,Q_t^2)=\tilde{f}^0(\omega,\gamma=\gamma_{gg}(\omega,\bar{\alpha}_s))\gamma_{gg}(\omega,\bar{\alpha}_s)R(\alpha_s,\omega)(Q_t^2)^{\gamma_{gg}(\omega,\bar{\alpha}_s)}, \quad (34)$$

where

$$R(\alpha_s,\omega)=-\left[\frac{\bar{\alpha}_s}{\omega}\gamma_{gg}(\omega,\bar{\alpha}_s)\frac{d\tilde{K}(\gamma)}{d\gamma}|_{\gamma=\gamma_{gg}(\omega,\bar{\alpha}_s)}\right]^{-1}. \quad (35)$$

The anomalous dimension will also, of course, control the large Q^2 behaviour of the moment function $\bar{g}(\omega,Q^2)$ of the integrated gluon distribution

$$\bar{g}(\omega,Q^2)=\int_0^{Q^2}\frac{dQ_t^2}{Q_t^2}f(\omega,Q_t^2), \quad (36)$$

which has the following form:

$$\bar{g}(\omega,Q^2)=R(\alpha_s,\omega)\bar{g}^0(\omega)\left(\frac{Q^2}{Q_0^2}\right)^{\gamma_{gg}(\omega,\bar{\alpha}_s)}, \quad (37)$$

where we have introduced the moment function of the input distribution

$$\bar{g}^0(\omega)=\tilde{f}^0(\omega,\gamma=\gamma_{gg}(\omega,\bar{\alpha}_s))(Q_0^2)^{\gamma_{gg}(\omega,\bar{\alpha}_s)}. \quad (38)$$

Equations (37) and (38) follow directly from equations (34), (35) and (36). It may be seen from Eq. (37) that the BFKL singularity affects through the factor R the "starting" gluon distribution at $Q^2=Q_0^2$ [22].

It follows from Eq. (31) that the anomalous dimension $\gamma_{gg}(\omega,\bar{\alpha}_s))$ is the solution of the following equation:

$$\frac{\bar{\alpha}_s}{\omega}\tilde{K}(\gamma_{gg}(\omega,\bar{\alpha}_s))=1. \quad (39)$$

It is a function of only one variable $\frac{\bar{\alpha}_s}{\omega}$ *i.e.* $\gamma_{gg}(\omega,\bar{\alpha}_s)\to\gamma_{gg}(\frac{\bar{\alpha}_s}{\omega})$. The solution of Eq. (39) makes it possible to obtain the anomalous dimension $\gamma_{gg}(\frac{\bar{\alpha}_s}{\omega})$ as a power series of $\frac{\bar{\alpha}_s}{\omega}$ [21]

$$\gamma_{gg}(\frac{\bar{\alpha}_s}{\omega})=\sum_{n=1}^{\infty}c_n\left(\frac{\bar{\alpha}_s}{\omega}\right)^n. \quad (40)$$

This power series corresponds to the leading $\ln(1/z)$ expansion of the splitting function $P_{gg}(z, \alpha_s)$

$$zP_{gg}(z, \alpha_s) = \bar{\alpha}_s \sum_{n=1}^{\infty} c_n \frac{(\bar{\alpha}_s \ln(1/z))^{n-1}}{(n-1)!} \tag{41}$$

which controls the evolution of the gluon distribution.

The exponent λ_{BFKL} controlling the small x behaviour of $f(x, Q_t^2)$ is

$$\lambda_{\mathrm{BFKL}} = \bar{\alpha}_s \tilde{K}(1/2). \tag{42}$$

The anomalous dimension has a branch point singularity at $\omega = \lambda_{\mathrm{BFKL}}$. We also have

$$\gamma_{gg}(\omega = \lambda_{\mathrm{BFKL}}) = \tfrac{1}{2}. \tag{43}$$

The following properties of the solution of the BFKL equation summarized in the formula (25) should be noted:

1. It exhibits the Regge type $x^{-\lambda}$ increase with decreasing x where the exponent $\lambda = \lambda_{\mathrm{BFKL}}$ can have potentially large magnitude $\approx 1/2$. The quantity $1 + \lambda_{\mathrm{BFKL}}$ is equal to the intercept of the so called BFKL pomeron which corresponds to the hard QCD interactions. Its potentially large magnitude (≈ 1.5) should be contrasted with the intercept $\alpha_{\mathrm{soft}} \approx 1.08$ of the effective "soft" pomeron which has been determined from the phenomenological analysis of the high energy behaviour of hadronic and photoproduction total cross-sections [9].
2. It exhibits the $(Q_t^2)^{1/2}$ growth with increasing Q_t^2 modulated by the Gaussian distribution in $\ln(Q_t^2)$ of width increasing as $\ln^{1/2}(1/x)$ with decreasing x. The Gaussian factor reflects the diffusion pattern inherent in the BFKL equation. The increase of the function $f(x, Q_t^2)$ as $(Q_t^2)^{1/2}$ is due to the fact that the leading twist anomalous dimension is equal to $1/2$ for $\omega = \lambda_{\mathrm{BFKL}}$ (see Eq. (43)). This shift of the anomalous dimension is the result of the (infinite) $LL1/x$ resumation.
3. The diffusion pattern of the solution of the BFKL equation is the direct consequence of the absence of transverse momentum ordering along the gluon chain. In this respect the BFKL dynamics is different from that based on the (leading order) Altarelli–Parisi evolution which corresponds to the strongly ordered transverse momenta. The interrelation between the diffusion of transverse momenta towards both the infrared and ultraviolet regions **and** the increase of gluon distributions with decreasing x is an important property of QCD at low x. It has important consequences for the structure of the hadronic final state in deep inelastic scattering at small x.

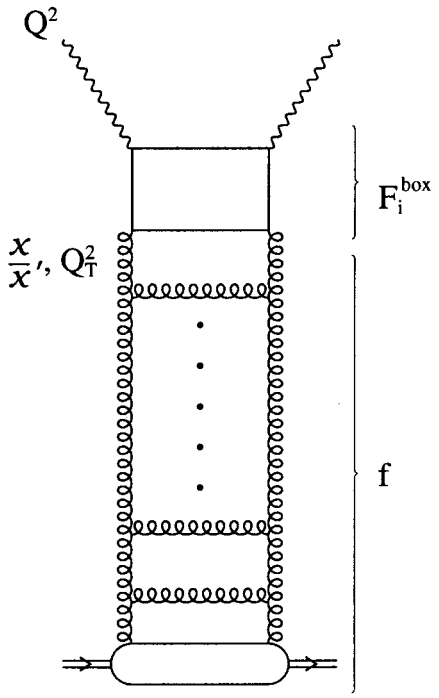

Fig. 5. Diagrammatic representation of the k_t factorization formula (44).

The structure functions $F_{2,L}(x, Q^2)$ are described at small x by the diagram of Fig. 5 which gives the following relation between the structure functions and the unintegrated distribution f:

$$F_{2,L}(x, Q^2) = \int_x^1 \frac{dx'}{x'} \int \frac{dQ_t^2}{Q_t^2} F_{2,L}^{\text{box}}(x', Q_t^2, Q^2) f(\frac{x}{x'}, Q_t^2) . \qquad (44)$$

The functions $F_{2,L}^{\text{box}}(x', Q_t^2, Q^2)$ may be regarded as the structure functions of the off-shell gluons with virtuality Q_t^2. They are described by the quark box (and crossed box) diagram contributions to the photon-gluon interaction in the upper part of the diagram of Fig. 5. The small x behaviour of the structure functions reflects the small z ($z = x/x'$) behaviour of the gluon distribution $f(z, Q_t^2)$.

The equation (44) is an example of the "k_t factorization theorem" which relates the measurable quantities (like DIS structure functions) to the convolution in both longitudinal as well as in transverse momenta of the universal gluon distribution $f(z, Q_t^2)$ with the cross-section (or structure function) describing the interaction of the "off-shell" gluon with the hard probe [22, 24].

The k_t factorization theorem is the basic tool for calculating the observable quantities in the small x region in terms of the (unintegrated) gluon distribution f which is the solution of the BFKL equation.

The leading-twist part of the k_t factorization formula can be rewritten in a collinear factorization form. The leading small x effects are then automatically resumed in the splitting functions and in the coefficient functions. The k_t factorization theorem can in fact be used as the tool for calculating these quantities. We shall demonstrate this using the example of the P_{qg} splitting function which is responsible for the evolution of the quark densities at low x (see Eqs () and (14)).

From the k_t factorization theorem we get:

$$Q^2 \frac{d\bar{F}_2(\omega, Q^2)}{dQ^2} = \int \frac{dQ_t^2}{Q_t^2} Q^2 \frac{d\bar{F}_2^{\text{box}}(\omega, Q_t^2, Q^2)}{dQ^2} \bar{f}(\omega, Q_t^2)\,, \tag{45}$$

where $\bar{F}_2(\omega, Q^2)$ and $\bar{F}_2^{\text{box}}(\omega, Q_t^2, Q^2)$ are the corresponding moment functions *i.e.*

$$\bar{F}_2(\omega, Q^2) = \int_0^1 \frac{dx}{x} x^\omega F_2(x, Q^2)\,, \tag{46}$$

and

$$\bar{F}_2^{\text{box}}(\omega, Q_t^2, Q^2) = \int_0^1 \frac{dx}{x} x^\omega F_2^{\text{box}}(x, Q_t^2, Q^2)\,. \tag{47}$$

Inserting the (inverse) Mellin representation of $\bar{F}_2^{\text{box}}(\omega, Q_t^2, Q^2)$

$$\bar{F}_2^{\text{box}}(\omega, Q_t^2, Q^2) = \frac{1}{2\pi i} \int_{1/2-i\infty}^{1/2+i\infty} d\gamma \tilde{F}_2^{\text{box}}(\omega, \gamma) \left(\frac{Q^2}{Q_t^2}\right)^\gamma\,, \tag{48}$$

and of $\bar{f}(\omega, Q_t^2)$ (see Eq. (33)) into Eq. (45) we get the following representation of $Q^2 \frac{d\bar{F}_2(\omega,Q^2)}{dQ^2}$

$$Q^2 \frac{d\bar{F}_2(\omega, Q^2)}{dQ^2} = \frac{1}{2\pi i} \int_{1/2-i\infty}^{1/2+i\infty} d\gamma\gamma \tilde{F}_2^{\text{box}}(\omega, \gamma) \tilde{f}(\omega, \gamma) (Q^2)^\gamma\,. \tag{49}$$

The leading twist part of the integral in Eq. (49) is controlled by the anomalous dimension $\gamma_{gg}(\frac{\bar{\alpha}_s}{\omega})$ which is a pole of $\tilde{f}(\omega, \gamma)$ in the complex γ plane.

It gives the following contribution to $Q^2\frac{d\bar{F}_2(\omega,Q^2)}{dQ^2}$:

$$Q^2\frac{d\bar{F}_2(\omega,Q^2)}{dQ^2}=\gamma_{gg}^2\left(\frac{\bar{\alpha}_s}{\omega}\right)\tilde{F}_2^{\mathrm{box}}\left(\omega,\gamma=\gamma_{gg}(\frac{\bar{\alpha}_s}{\omega})\right)g(\omega,Q^2)\,, \tag{50}$$

where we have taken into account equations (34), (37) and (38). In the so-called DIS scheme the QCD-improved parton model relation (5) holds beyond the leading order and so we have the following relation between $Q^2\frac{d\bar{F}_2(\omega,Q^2)}{dQ^2}$ and $g(\omega,Q^2)$

$$Q^2\frac{d\bar{F}_2(\omega,Q^2)}{dQ^2}=2\sum_i e_i^2 P_{qg}(\omega,\alpha_s)g(\omega,Q^2)+\ldots\,, \tag{51}$$

where $P_{qg}(\omega,\alpha_s)$ is the moment of the splitting function $P_{qg}(z,\alpha_s)$. Comparing Eq. (51) with (50) we get the following prescription for $P_{qg}(\omega,\alpha_s)$ in the leading $\ln(1/x)$ (or rather in the leading $1/\omega$) approximation [24, 25]:

$$P_{qg}(\omega,\alpha_s)=\frac{\gamma_{gg}^2(\frac{\bar{\alpha}_s}{\omega})\tilde{F}_2^{\mathrm{box}}\left(\omega=0,\gamma=\gamma_{gg}(\frac{\bar{\alpha}_s}{\omega})\right)}{2\sum_i e_i^2}\,. \tag{52}$$

The function $\gamma^2\tilde{F}_2^{\mathrm{box}}(\omega=0,\gamma)$ can be expanded into the following power series in γ

$$\gamma^2\tilde{F}_2^{\mathrm{box}}(\omega=0,\gamma)=\bar{\alpha}_s(d_0+\sum_{n=1}^{\infty}d_n\gamma^n)\,. \tag{53}$$

It should be noted that the function $\tilde{F}_2^{\mathrm{box}}(\omega=0,\gamma)$ has the $1/\gamma^2$ singularity at $\gamma=0$. This follows from the fact that $\tilde{F}_2^{\mathrm{box}}(\omega,Q_t^2,Q^2)\sim\ln(Q^2/Q_t^2)$ at large Q^2/Q_t^2 because of the collinear singularity. The function $\gamma^2\tilde{F}_2^{\mathrm{box}}(\omega=0,\gamma)$ is regular at $\gamma=0$ and can be expanded in the power series (53).

From the power series (53) we get the following expansion:

$$\gamma_{gg}^2\left(\frac{\bar{\alpha}_s}{\omega}\right)\tilde{F}_2^{\mathrm{box}}\left(\omega=0,\gamma=\gamma_{gg}\left(\frac{\bar{\alpha}_s}{\omega}\right)\right)=\bar{\alpha}_s\left[d_0+\sum_{n=1}^{\infty}d_n\gamma_{gg}^n\left(\frac{\bar{\alpha}_s}{\omega}\right)\right]\,. \tag{54}$$

Combining this expansion with the expansion (40) of the anomalous dimension $\gamma_{gg}(\frac{\bar{\alpha}_s}{\omega})$ we get the following expansion of the splitting function $P_{qg}(z,\alpha_s)$ at small z:

$$zP_{qg}(z,\alpha_s)=\frac{\alpha_s}{2\pi}zP^{(0)}(z)+(\bar{\alpha}_s)^2\sum_{n=1}^{\infty}b_n\frac{[\bar{\alpha}_s\ln(1/z)]^{n-1}}{(n-1)!}\,, \tag{55}$$

where the coefficients b_n can be expressed in terms of c_n and d_n appearing in the expansions (40) and (53), respectively. The first term on the right hand side of Eq. (55) vanishes at $z = 0$. It should be noted that the splitting function P_{qg} when compared with the splitting function P_{gg} is formally non-leading at small z. For moderately small values of z however, when the first few terms in the expansions (40) and (55) dominate, the BFKL effects can be much more important in P_{qg} than in P_{gg}. This comes from the fact that in the expansion (55) all coefficients b_n are different from zero while in Eq. (40) we have $c_2 = c_3 = 0$ [21]. The small x resumation effects within the conventional QCD evolution formalism have recently been discussed in Refs [26–29].

A more general treatment of the gluon ladder than that which follows from the BFKL formalism is provided by the CCFM equation based on angular ordering along the gluon chain [16, 17]. This equation embodies both the BFKL equation at small x and the conventional Altarelli–Parisi evolution at large x. The unintegrated gluon distribution f now acquires dependence upon an additional scale Q which specifies the maximal angle of gluon emission. The CCFM equation has a form analogous to that of the "folded" BFKL equation (22):

$$f(x,Q_t^2,Q^2) = \hat{f}^0(x,Q_t^2,Q^2) + \bar{\alpha}_s \int_x^1 \frac{dx'}{x'} \int \frac{d^2q}{\pi q^2} \Theta(Q - qx/x')$$

$$\times \Delta_R(\frac{x}{x'},Q_t^2,q^2) \frac{Q_t^2}{(q+Q_t)^2} f(x',(q+Q_t)^2,q^2)), \tag{56}$$

where the theta function $\Theta(Q - qx/x')$ reflects the angular ordering constraint on the emitted gluon. The "non-Sudakov" form-factor $\Delta_R(z,Q_t^2,q^2)$ is now given by the following formula:

$$\Delta_R(z,Q_t^2,q^2) = \exp\left[-\bar{\alpha}_s \int_z^1 \frac{dz'}{z'} \int \frac{dq'^2}{q'^2} \Theta(q'^2 - (qz')^2) \Theta(Q_t^2 - q'^2)\right]. \tag{57}$$

Eq. (56) still contains only the singular term of the $g \to gg$ splitting function at small z. Its generalization which would include remaining parts of this vertex (as well as quarks) is possible.

In Fig. 6 we show the results for the structure function F_2 calculated from the k_t factorization theorem using the function f obtained from the CCFM equation [30]. We confront these predictions with the most recent data from the H1 and ZEUS collaborations at HERA [7, 8] as well as with the results of the analysis which was based on the Altarelli–Parisi equation

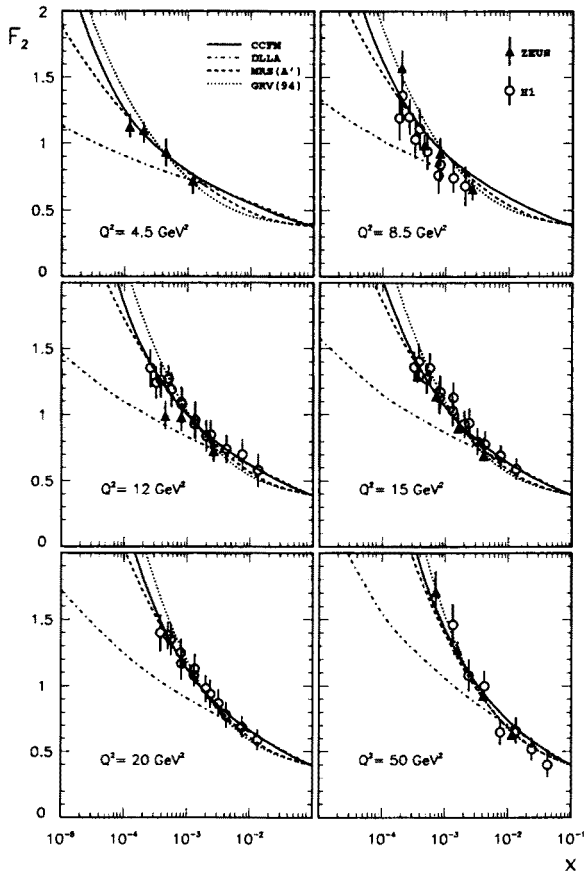

Fig. 6. A comparison of the HERA measurements of F_2 [7, 8] with the predictions based on the k_t factorization formula (44) using for the unintegrated gluon distributions f the solutions of the CCFM equation (56) (continuous curve) and of the approximate form of this equation corresponding to setting $\Theta(Q-q)$ in place of $\Theta(Q-qx/x')$ and $\Delta_R = 1$ (dotted curve). We also show the values of F_2 obtained from collinear factorization using the MRS(A') [31] and GRV [32] partons (the figure is taken from Ref. [30]).

alone without the small x resumation effects being included in the formalism [31, 32]. In the latter case the singular small x behaviour of the gluon and sea quark distributions has to be introduced in a parametrization of the starting distributions at the moderately large reference scale $Q^2 = Q_0^2$ (*i.e.* $Q_0^2 \approx 4GeV^2$ or so) [31]. One can also generate steep behaviour dynamically starting from the non-singular "valence-like" parton distributions at some very low scale $Q_0^2 = 0.35GeV^2$ [32]. In the latter case the gluon and sea

quark distributions exhibit "double logarithmic behaviour" (18). For very small values of the scale Q_0^2 the evolution length $\xi(Q^2, Q_0^2)$ can become large for moderate and large values of Q^2 and the "double logarithmic" behaviour (18) is, within the limited region of x, similar to that corresponding to the power like increase of the type $x^{-\lambda}$, $\lambda \approx 0.3$. This explains similarity between the theoretical curves presented in Fig. 6. The theoretical results also show that an inclusive quantity like F_2 is not the best discriminator for revealing the dynamical details at low x. One may however hope that this can be provided by studying the structure of the hadronic final state in deep inelastic scattering and this possibility will be briefly discussed in the next section.

5. The structure of the hadronic final state in deep inelastic scattering at low x

It is expected that absence of transverse momentum ordering along the gluon chain which leads to the correlation between the increase of the structure function with decreasing x and the diffusion of transverse momentum should reflect itself in the behaviour of less inclusive quantities than the structure function $F_2(x, Q^2)$. The dedicated measurements of the low x physics which are particularly sensitive to this correlation are the deep inelastic plus jet events, transverse energy flow in deep inelastic scattering, production of jets separated by the large rapidity gap and dijet production in deep inelastic scattering. The diagrammatic illustration of these measurements is presented in Fig. 7.

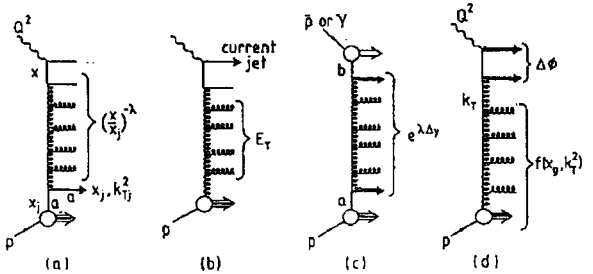

Fig. 7. Diagrammatic representation of the processes testing the BFKL dynamics. (a) Deep inelastic scattering with the forward jet. (b) E_T flow in deep inelastic scattering. (c) Production of jets separated by the large rapidity gap Δy. (d) Dijet production in deep inelastic scattering (the figure is taken from Ref. [33]).

In principle deep inelastic lepton scattering containing a measured jet can provide a very clear test of the BFKL dynamics at low x [34, 35, 37]. The

idea is to study deep inelastic (x, Q^2) events which contain an identified jet (x_j, k_{Tj}^2) where $x \ll x_j$ and $Q^2 \approx k_{Tj}^2$. Since we choose events with $Q^2 \approx k_{Tj}^2$ the leading order QCD evolution (from k_{Tj}^2 to Q^2) is neutralized and attention is focussed on the small x, or rather small x/x_j behaviour. The small x/x_j behaviour of jet production is generated by the gluon radiation as shown in the diagram of Fig. 7a. Choosing the configuration $Q^2 \approx k_{Tj}^2$ we eliminate by definition gluon emission which corresponds to strongly ordered transverse momenta *i.e.* that emission which is responsible for the LO QCD evolution. The measurement of jet production in this configuration may, therefore, test more directly the $(x/x_j)^{-\lambda}$ behaviour which is generated by the BFKL equation where the transverse momenta are not ordered. The recent H1 results concerning deep inelastic plus jest events are consistent with the increase of the cross-section with decreasing x as predicted by the BFKL dynamics [38].

Conceptually similar process is that of the two-jet production separated by a large rapidity gap Δy in hadronic collisions or in photoproduction as illustrated in Fig. 7c [39, 40]. Besides the characteristic $\exp(\lambda \Delta y)$ dependence of the two-jet cross-section one expects significant weakening of the azimuthal back-to-back correlations of the two jets. This is the direct consequence of the absence of transverse momentum ordering along the gluon chain in the diagram of Fig. 7c.

Another measurement which should be sensitive to the QCD dynamics at small x is that of the transverse energy flow in deep inelastic lepton scattering in the central region away from the current jet and from the proton remnant as illustrated in Fig. 7b. [41]. The BFKL dynamics predicts in this case a substantial amount of transverse energy which should increase with decreasing x. The experimental data are consistent with this theoretical expectation [38]. Absence of transverse momentum ordering also implies weakening of the back-to-back azimuthal correlation of dijets produced close to the photon fragmentation region (see Fig. 7d) [42, 43].

Another important process which is sensitive to the small x dynamics is the deep inelastic diffraction [44, 45]. Deep inelastic diffraction in ep inelastic scattering is a process:

$$e(p_e) + p(p) \to e'(p_e') + X + p'(p'), \tag{58}$$

where there is a large rapidity gap between the recoil proton (or excited proton) and the hadronic system X (see Fig. 8a). To be precise process (58) reflects the diffractive dissociation of the virtual photon. Diffractive dissociation is described by the following kinematical variables:

$$\beta = \frac{Q^2}{2(p - p')q}, \tag{59}$$

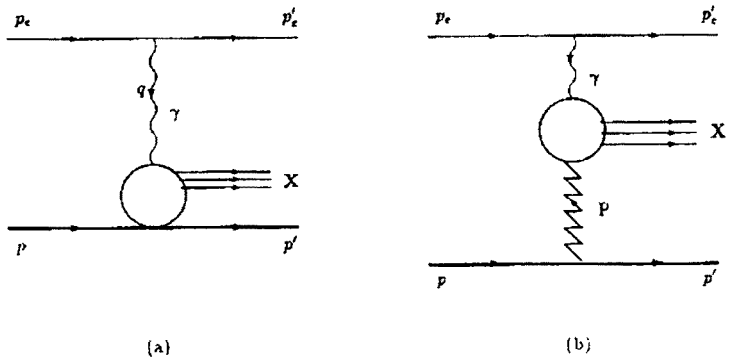

Fig. 8. (a) Kinematics of the large rapidity gap processes $e+p \to e'+X+p'$. The wavy line represents the virtual photon. (b) The pomeron exchange diagram for diffractive production of the hadronic system X by a virtual photon. The wavy and zigzag lines represent the virtual photon and pomeron, respectively.

$$x_P = \frac{x}{\beta}, \tag{60}$$

$$t = (p - p')^2 . \tag{61}$$

Assuming that diffraction dissociation is dominated by the pomeron exchange as shown in Fig. 8b and that the pomeron is described by a Regge pole one gets the following factorizable expression for the diffractive structure function [47–49, 52, 50]:

$$\frac{\partial F_2^{\text{diff}}}{\partial x_P \partial t} = f(x_P, t) F_2^P(\beta, Q^2, t) , \tag{62}$$

where the "flux factor" $f(x_P, t)$ is given by the following formula:

$$f(x_P, t) = N \frac{B^2(t)}{16\pi} x_P^{1-2\alpha_P(t)} \tag{63}$$

with $B(t)$ describing the pomeron coupling to a proton and N being the normalization factor. The function $F_2^P(\beta, Q^2, t)$ is the pomeron structure function which in the (QCD improved) parton model is related in a standard way to the quark and antiquark distribution functions in a pomeron (see Fig. 9).

$$F_2^P(\beta, Q^2, t) = \beta \sum e_i^2 [q_i^P(\beta, Q^2, t) + \bar{q}_i^P(\beta, Q^2, t)] \tag{64}$$

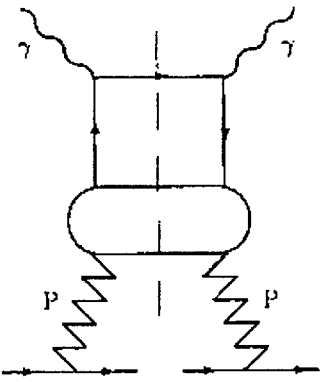

Fig. 9. The hand-bag diagram for the virtual Compton diffractive production. The wavy and zigzag lines represent the virtual photon and pomeron, respectively.

with $q_i^P(\beta, Q^2, t) = \bar{q}_i^P(\beta, Q^2, t)$. The variable β which is the Bjorken scaling variable appropriate for deep inelastic lepton-pomeron "scattering", has the meaning of the momentum fraction of the pomeron carried by the probed quark (antiquark). The quark distributions in a pomeron are assumed to obey the standard Altarelli–Parisi evolution equations:

$$Q^2 \frac{\partial q^P}{\partial Q^2} = P_{qq} \otimes q^P + P_{qg} \otimes g^P \tag{65}$$

with a similar equation for the evolution of the gluon distribution in a pomeron. The first term on the right hand side of the Eq. (65) becomes negative at large β, while the second term remains positive and is usually very small at large β unless the gluon distributions are large and have a hard spectrum.

In Figs. 10a,b we show the theoretical results for the quantity

$$F_2^D(\beta, Q^2) = \int_{x_{PL}}^{x_{PH}} dx_P \int_{-\infty}^{0} dt \frac{\partial F_2^{\text{diff}}}{\partial x_P \partial t} \tag{66}$$

with $x_{PL} = 0.0003$ and $x_{PH} = 0.05$ based on the "conventional" parton distributions in a pomeron vanishing as $(1-\beta)$ at $\beta = 1$ and compare these results with the experimental data from HERA [46]. The data suggest that the slope of F_2^P as the function of Q^2 does not change sign even at relatively large values of β. This favours the hard gluon spectrum in a pomeron [53, 54], and should be contrasted with the behaviour of the structure function of the proton which, at large x, decreases with increasing Q^2. The data

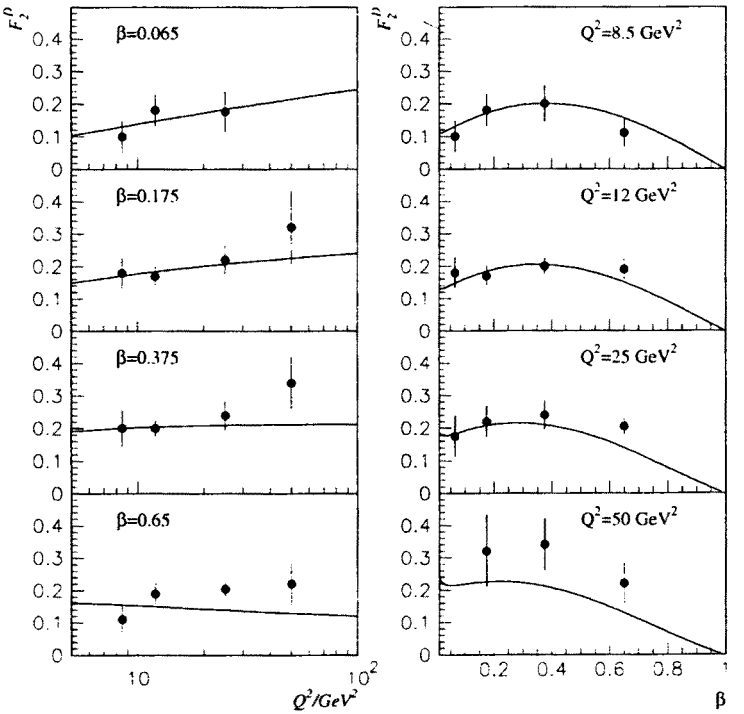

Fig. 10. Theoretical predictions based on the soft pomeron exchange with low intercept $\alpha_{\text{soft}} = 1.1$ [50, 51] for the diffractive structure function $F_2^{D(3)}(x_P, \beta, Q^2)$ defined by Eq. (67) and their comparison with the data from HERA [46].

on inclusive diffractive production favour the soft pomeron with relatively low intercept. This is illustrated in Fig. 11 where we plot the theoretical prediction for the quantity

$$F_2^{D(3)}(x_P, \beta, Q^2) = \int_{-\infty}^{0} dt \frac{\partial F_2^{\text{diff}}}{\partial x_P \partial t}, \tag{67}$$

based on the "soft" pomeron with low intercept $\alpha_{\text{soft}} = 1.1$ and compare these predictions with the experimental data from HERA [46]. The diffractive production of vector mesons seems to require a "hard" pomeron contribution [55–57] . It has also been pointed out that the factorization property (62) may not hold in models based entirely on perturbative QCD when the pomeron is represented by the BFKL ladder [58, 59]. There exist also models of deep inelastic diffraction which do not rely on the pomeron exchange

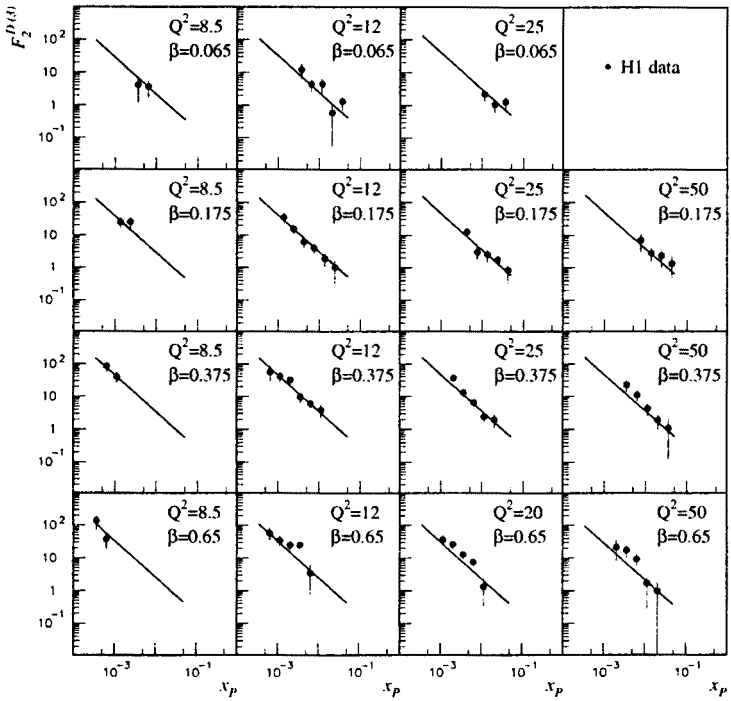

Fig. 11. Theoretical predictions [50, 51] for the diffractive structure function $F_2^D(\beta, Q^2)$ defined by Eq. (66) and their comparison with the data from HERA [46]. The structure function $F_2^D(\beta, Q^2)$ is plotted (a) as the function of Q^2 for fixed values of β and (b) as the function of β for fixed values of Q^2. The figure is taken from Ref. [50].

picture [60, 61].

The structure function $F_2^{D(3)}(x_P, \beta, Q^2)$ is plotted as the function of x_p for different values of β and Q^2.

6. Summary and conclusions

In this lecture we have briefly described the QCD expectations for deep inelastic lepton scattering at low x which follow from the BFKL dynamics. It leads to the indefinite increase of gluon distributions with decreasing x which is correlated with the diffusion of transverse momenta. This increase of gluon distribution implies a similar increase of the structure functions through the $g \to q\bar{q}$ transitions. Besides discussing the theoretical and phenomenological issues related to the description of the structure function

F_2 at low x we have also emphasized the role of studying the hadronic final state in deep inelastic scattering.

The indefinite growth of parton distributions cannot go on forever and has to be eventually stopped by parton screening which leads to the parton saturation. Most probably however the saturation limit is still irrelevant for the small x region which is now being probed at HERA.

We have limited ourselves to the large Q^2 region where perturbative QCD is expected to be applicable. Specific problems of the low Q^2, low x region are discussed in Ref. [62]. Finally, let us point out that the change of the dynamics with the relevant scale is clearly visible in the data (see Fig. 2) and its satisfactory explanation is perhaps one of the most challenging problems of to-day.

I thank the organizers of the Jubilee XXXV Cracow School of Theoretical Physics for organizing an excellent meeting. I thank Barbara Badełek, Krzysztof Golec–Biernat, Alan Martin and Peter Sutton for most enjoyable research collaborations on the problems presented in this lecture. I am grateful to Grey College and to Physics Department of the University of Durham for their warm hospitality.

REFERENCES

[1] L.N. Gribov, E.M. Levin, M.G. Ryskin, *Phys. Rep.* **100**, 1 (1983).
[2] B. Badełek *et al.*, *Rev. Mod. Phys.* **64**, 927 (1992).
[3] A.D. Martin, Acta Phys. Pol. **B25**, 265 (1994).
[4] J. Kwieciński, *Nucl. Phys. B* (Proc. Suppl.) **39 B,C**, 58 (1995).
[5] E.A. Kuraev, L.N. Lipatov, V.Fadin, *Zh. Eksp. Teor. Fiz.* **72**, 373 (1977) (*Sov. Phys. JETP* **45**, 199 (1977)); Ya.Ya. Balitzkij, L.N. Lipatov, *Yad. Fiz.* **28**, 1597 (1978) (*Sov. J. Nucl. Phys.* **28**, 822 (1978)); L.N. Lipatov, in *Perturbative QCD*, edited by A.H. Mueller, World Scientific, Singapore 1989, p. 441; J.B. Bronzan, R.L. Sugar, *Phys. Rev.* **D17**, 585 (1978); T. Jaroszewicz, *Acta Phys. Pol.* **B11**, 965 (1980).
[6] A.J. Askew *et al.*, *Phys. Rev.* **D47**, 3775 (1993); *Phys. Rev.* **D49**, 4402 (1994).
[7] H1 collaboration: A. de Roeck *et al.*, preliminary measurements to be published in the Proc. of the Workshop on DIS and QCD, Paris 1995, DESY preprint 95–152.
[8] ZEUS collaboration: B. Foster, to be published in the Proc. of the Workshop on DIS and QCD, Paris 1995, DESY preprint 95–193.
[9] A. Donnachie, P.V. Landshoff, *Phys. Lett.* **B296**, 257 (1992).
[10] P.D.B. Collins, *An Introduction to Regge Theory and High Energy Physics*, Cambridge University Press, Cambridge 1977.
[11] A. Donnachie, P.V. Landshoff, *Z. Phys.* **C61**, 161 (1994).

[12] A. Levy, talk given at the UK Phenomenology Workshop on HERA Physics, St. John's College, Durham, UK, September 1995.
[13] G. Altarelli, G. Parisi, *Nucl. Phys.* **B126**, 298 (1977).
[14] E. Reya, *Phys. Rep.* **69**, 195 (1981); G. Altarelli, *Phys. Rep.* **81**, 1 (1982).
[15] M. Ciafaloni, *Nucl. Phys.* **B296**, 49 (1988).
[16] S. Catani, F. Fiorani, G. Marchesini, *Phys. Lett.* **B234**, 339 (1990); *Nucl. Phys.* **B336**, 18 (1990); G. Marchesini, in Proceedings of the Workshop *QCD at 200 TeV*, Erice, Italy, 1990, edited by. L. Cifarelli and Yu. L. Dokshitzer, Plenum Press, New York 1992, p. 183; G. Marchesini, *Nucl. Phys.* **B445**, 49 (1995).
[17] J. Kwieciński, A.D. Martin, P.J. Sutton, *Phys. Rev.* **D52**, 1445 (1995).
[18] F. Halzen, A.D. Martin, *Quarks and Leptons: An Introductory Course in Modern Particle Physics*, John Wiley and Sons, 1984.
[19] R.G. Roberts, *The Structure of the Proton*, Cambridge University Press, 1990.
[20] P.V. Landshoff, J.C. Polkinghorne, K.D. Short, *Nucl. Phys.* **28**, 225 (1971).
[21] T. Jaroszewicz, *Phys. Lett.* **B116**, 291 (1982).
[22] M. Ciafaloni, *Phys. Lett.* **356**, 74 (1995).
[23] A.D. Martin, J. Kwieciński, P.J. Sutton, *Nucl. Phys. B* (Proc. Suppl.) **A29**, 67 (1992).
[24] S. Catani, M. Ciafaloni, F. Hautmann, *Phys. Lett.* **B242**, 97 (1990); *Nucl. Phys.* **B366**, 657 (1991); J.C. Collins, R.K. Ellis, *Nucl. Phys.* **B360**, 3 (1991); S. Catani, F. Hautmann, *Nucl. Phys.* **B427**, 000 (1994).
[25] J. Kwieciński, A.D. Martin, *Phys. Lett.* **B353**, 123 (1995).
[26] R.K. Ellis, Z. Kunszt, E.M. Levin, *Nucl. Phys.* **B420**, 517 (1994); Erratum-ibid; **B433**, 498 (1995).
[27] R.K. Ellis, F. Hautmann, B.R. Webber, *Phys. Lett.* **B348**, 582 (1995).
[28] R.D. Ball, S. Forte, *Phys. Lett.* **351**, 313 (1995).
[29] J.R. Forshaw, R.G. Roberts, R.S. Thorne, *Phys. Lett.* **B356**, 79 (1995).
[30] J. Kwieciński, A.D.Martin, P.J. Sutton, Durham preprint DTP/95/94.
[31] A.D. Martin, R.G. Roberts, W.J. Stirling, *Phys. Rev.* **D50**, 6734 (1994); *Phys. Lett.* **354**, 155 (1995).
[32] M. Glück, E. Reya, A. Vogt, *Z. Phys.* **C67**, 433 (1995).
[33] A.D. Martin, review talk presented at the Blois Workshop *The Heart of the Matter*, June 1994, Blois, France.
[34] A.H. Mueller, *J. Phys.* **G17**, 1443 (1991).
[35] J. Bartels, M. Loewe, A. DeRoeck, *Z. Phys.* **C54**, 635 (1992).
[36] W.K.Tang, *Phys. Lett.* **B278**, 363 (1992).
[37] J. Kwieciński, A.D. Martin, P.J. Sutton, *Phys. Rev.* **D46**, 921 (1992); *Phys. Lett.* **B287**, 254 (1992).
[38] H1 Collaboration, DESY preprint 95-108.
[39] V. del Duca, *Phys. Rev.* **D49**, 4510 (1994).
[40] W.J. Stirling, *Nucl. Phys.* **B423**, 56 (1994).
[41] J. Kwieciński, A.D. Martin, P.J. Sutton, K.Golec–Biernat, *Phys. Rev.* **D50**, 217 (1994); K.Golec-Biernat, J. Kwieciński, A.D. Martin, P.J. Sutton, *Phys. Lett.* **B335**, 220 (1994).

[42] J.R. Forshaw, R.G. Roberts, RAL preprint 94-0228.
[43] A.J. Askew *et al.*, *Phys. Lett.* **B338**, 92 (1994).
[44] ZEUS Collaboration, M. Derrick *et al.*, *Phys. Lett.* **B315**, 481 (1993); **332**, 228 (1994); **B338**, 483 (1994).
[45] H1 Collaboration, T. Ahmed *et al.*, *Nucl. Phys.* **B 429**, 477 (1994).
[46] H1 Collaboration, T. Ahmed *et al.*, *Phys. Lett.* **B348**, 681 (1995).
[47] A. Donnachie, P.V. Landshoff, *Nucl. Phys.* **B244**, 322 (1984); **B267**, 690 (1986); *Phys. Lett.* **B191**, 000 (1987); **B198**, 590(E) (1987).
[48] A. Capella *et al.*, *Phys. Lett.* **B343**, 403 (1995).
[49] J.C. Collins *et al.*, *Phys. Rev.* **D51**, 3182 (1995).
[50] K. Golec–Biernat, J. Kwieciński, *Phys. Lett.* **B353**, 329 (1995).
[51] K. Golec–Biernat, to be published in the Proc. of the Workshop on DIS and QCD, Paris 1995.
[52] T. Gehrmann, W.J. Stirling, Durham preprint DTP/95/26.
[53] H. Abramowicz, talk given at the International Conference on Elastic and Diffractive Scattering, *Frontiers in Strong Interactions*, Chateau de Blois, France, June 1995.
[54] J. Dainton, talk given at the International Conference on Elastic and Diffractive Scattering, *Frontiers in Strong Interactions*, Chateau de Blois, France, June 1995.
[55] S. Donnachie, talk given at the International Conference on Elastic and Diffractive Scattering, *Frontiers in Strong Interactions*, Chateau de Blois, France, June 1995.
[56] J. Whitmore, talk given at the International Conference on Elastic and Diffractive Scattering, *Frontiers in Strong Interactions*, Chateau de Blois, France, June 1995.
[57] I. Kenyon, talk given at the International Conference on Elastic and Diffractive Scattering, *Frontiers in Strong Interactions*, Chateau de Blois, France, June 1995.
[58] N.N. Nikolaev, B.G. Zakharov, *Z. Phys.* **C53**,331 (1992); Jülich preprint KFA–IKP (TH)–1993–17; M. Genovesse, N.N. Nikolaev, B.G. Zakharov, Jülich preprint KFA–IKP (TH)–1994–307 (Torino preprint DFTT 42/94).
[59] E. Levin, M. Wüsthoff, *Phys. Rev.* **D50**, 4306 (1994); J. Bartels, H. Lotter, M. Wüsthoff, DESY preprint 94-95.
[60] W. Buchmüller, *Phys. Lett.* **B353**, 335 (1995).
[61] A. Edin, G. Ingelman, J. Rathsman, to be published in the Proc. of the Workshop on DIS and QCD, Paris 1995.
[62] B. Badełek, J. Kwieciński, Warsaw preprint IFD/1/94 (to appear in *Rev. Mod. Phys.*).